

**On
Steepest-Descent-Kaczmarz
Methods for Regularizing
Systems of Nonlinear
Ill-posed**

**A. De Cezaro, M. Haltmeier, A. Leitao, O.
Scherzer**

RICAM-Report 2008-03

On Steepest-Descent-Kaczmarz Methods for Regularizing Systems of Nonlinear Ill-posed Equations

A. De Cezaro[†] M. Haltmeier[‡] A. Leitão[§] O. Scherzer[‡]

January 24, 2008

Abstract

We investigate modified steepest descent methods coupled with a loping Kaczmarz strategy for obtaining stable solutions of nonlinear systems of ill-posed operator equations. We show that the proposed method is a convergent regularization method. Numerical tests are presented for a linear problem related to photoacoustic tomography and a non-linear problem related to the testing of semiconductor devices.

Keywords. Nonlinear systems; Ill-posed equations; Regularization; Steepest descent method; Kaczmarz method.

AMS Classification: 65J20, 47J06.

1 Introduction

In this paper we propose a new method for obtaining regularized approximations of systems of nonlinear ill-posed operator equations.

The *inverse problem* we are interested in consists of determining an unknown physical quantity $x \in X$ from the set of data $(y_0, \dots, y_{N-1}) \in Y^N$, where X, Y are Hilbert spaces and $N \geq 1$. In practical situations, we do not know the data exactly. Instead, we have only approximate measured data $y_i^\delta \in Y$ satisfying

$$\|y_i^\delta - y_i\| \leq \delta^i, \quad i = 0, \dots, N-1, \quad (1)$$

[†]IMPA, Estr. D. Castorina 110, 22460-320 Rio de Janeiro, Brazil decezar@impa.br.

[‡]Department of Computer Science, University of Innsbruck, Technikerstrasse 21a, A-6020 Innsbruck, Austria markus.haltmeier@uibk.ac.at, otmar.scherzer@uibk.ac.at.

[§]Department of Mathematics, Federal University of St. Catarina, P.O. Box 476, 88040-900 Florianópolis, Brazil aleitao@mtm.ufsc.br.

with $\delta^i > 0$ (noise level). The finite set of data above is obtained by indirect measurements of the parameter, this process being described by the model

$$F_i(x) = y^i, \quad i = 0, \dots, N-1, \quad (2)$$

where $F_i : D_i \subset X \rightarrow Y$, and D_i are the corresponding domains of definition.

Standard methods for the solution of system (2) are based in the use of *Iterative type* regularization methods [1, 7, 13, 16, 19]) or *Tikhonov type* regularization methods [7, 23, 30, 33, 32] after rewriting (2) as a single equation $F(x) = y$, where

$$F := (F_0, \dots, F_{N-1}) : \bigcap_{i=0}^{N-1} D_i \rightarrow Y^N \quad (3)$$

and $y := (y^0, \dots, y^{N-1})$. However these methods become inefficient if N is large or the evaluations of $F_i(x)$ and $F'_i(x)^*$ are expensive. In such a situation, Kaczmarz type methods [6, 15, 22, 25] which cyclically consider each equation in (2) separately are much faster [26] and are often the method of choice in practice.

For recent analysis of Kaczmarz type methods for systems of ill-posed equations, we refer the reader to [4, 10, 11, 17].

The starting point of our approach is the steepest descent method [7, 29] for solving ill-posed problems. Motivated by the ideas in [10, 11], we propose in this article a *loping Steepest-Descent-Kaczmarz method* (L-SDK method) for the solution of (2). This iterative method is defined by

$$x_{k+1}^\delta = x_k^\delta - \omega_k \alpha_k s_k, \quad (4)$$

where

$$s_k := F'_{[k]}(x_k^\delta)^*(F_{[k]}(x_k^\delta) - y_{[k]}^\delta), \quad (5)$$

$$\omega_k := \begin{cases} 1 & \|F_{[k]}(x_k^\delta) - y_{[k]}^\delta\| \geq \tau \delta_{[k]} \\ 0 & \text{otherwise} \end{cases}, \quad (6)$$

$$\alpha_k := \begin{cases} \Phi_{\text{rel}} \left(\|s_k\|^2 / \|F'_{[k]}(x_k^\delta) s_k\|^2 \right) & \omega_k = 1 \\ \alpha_{\text{min}} & \omega_k = 0 \end{cases}. \quad (7)$$

Here $\alpha_{\text{min}} > 0$, $\tau \in [2, \infty)$ are appropriate chosen numbers (see (13), (14) below), $[k] := (k \bmod N) \in \{0, \dots, N-1\}$, and $x_0^\delta = x_0 \in X$ is an initial guess, possibly incorporating some *a priori* knowledge about the exact solution. The function $\Phi_{\text{rel}} : (0, \infty) \rightarrow (0, \infty)$ defines a sequence of relaxation parameters and is assumed to be continuous, monotonically increasing, bounded by a constant α_{max} , and to satisfy $\Phi(s) \leq s$ (see Figure 1).

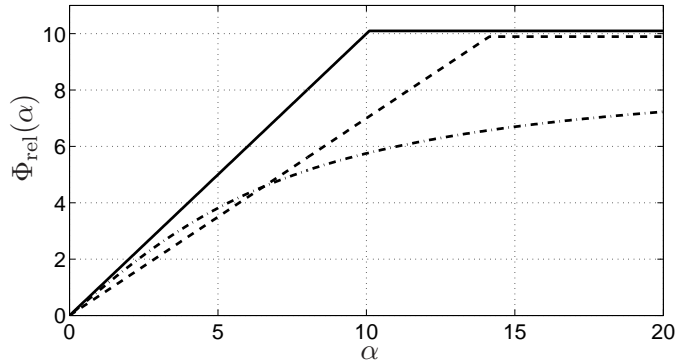


Figure 1: Typical examples for relaxation function Φ_{rel} .

If M is an upper bound for $\|F'_{[k]}(x)\|$, then $\|s_k\|^2/\|F'_{[k]}(x_k^\delta)s_k\|^2 \geq 1/M^2$ (cf. Lemma 3.2). Hence the relaxation function Φ_{rel} needs only be defined on $[1/M^2, \infty)$. In particular, if one chooses $\Phi_{\text{rel}}(s) = \alpha_{\min} \leq 1/M^2$ on that interval, then $\alpha_k = \alpha_{\min} \leq 1/M^2$ and the L-SDK method reduces to the loping Landweber-Kaczmarz (L-LK) method considered in [11, 10]. Note that the convergence of the L-LK method requires $\alpha_k \leq 1/M^2$, whereas the analysis in the present paper allows the relaxation parameters α_k to be much larger than $1/M^2$.

The L-SDK method consists in incorporating the Kaczmarz strategy (with the loping parameters ω_k) in the steepest descent method. This strategy is analog to the one introduced in [11] regarding the Landweber-Kaczmarz iteration. As usual in Kaczmarz-type algorithms, a group of N subsequent steps (starting at some multiple k of N) shall be called a *cycle*. The iteration should be terminated when, for the first time, all x_k are equal within a cycle. That is, we stop the iteration at

$$k_*^\delta := \arg \min \{lN \in \mathbb{N} : x_{lN} = x_{lN+1} = \dots = x_{lN+N-1}\}, \quad (8)$$

Notice that k_*^δ is the smallest multiple of N such that

$$x_{k_*^\delta} = x_{k_*^\delta+1} = \dots = x_{k_*^\delta+N-1}. \quad (9)$$

In the case of noise free data, $\delta^i = 0$ in (1), we choose $\omega_k \equiv 1$ and the iteration (4) - (7) reduces to the *Steepest-Descent-Kaczmarz* (SDK) method, which is closely related to the *Landweber-Kaczmarz* (LK) method considered in [17].

It is worth noticing that, for noisy data, the L-SDK method is fundamentally different from the SDK method: The bang-bang relaxation parameter ω_k effects that the iterates defined in (4) become stationary if *all components* of the residual vector $\|F_i(x_k^\delta) - y^{\delta,i}\|$ fall below a pre-specified threshold. This

characteristic renders (4) – (7) a regularization method (see Section 3). Another consequence of using these relaxation parameters is the fact that, after a large number of iterations, ω_k will vanish for some k within each iteration cycle. Therefore, the computationally expensive evaluation of $F'_{[k]}(x_k)^*$ might be loped, making the LSDK method in (4) - (7) a fast alternative to the LK method in [17]. Since in praxis the steepest descent method performs better than the Landweber method, the L-SDK is expected to be more efficient than the L-LK method [10, 11]. Our numerical experiments (mainly for the nonlinear problem in Section 5) corroborate this conjecture.

The article is outlined as follows. In Section 2 we formulate basic assumptions and derive some auxiliary estimates required for the analysis. In Section 3 we provide a convergence analysis for the L-SDK method. In Sections 4 and 4 we compare the numerical performance of the L-SDK method with other standard methods for inverse problems in photoacoustic tomography and in semiconductors respectively.

2 Assumptions and Basic Results

We begin this section by introducing some assumptions, that are necessary for the convergence analysis presented in the next section. These assumptions derive from the classical assumptions used in the analysis of iterative regularization methods [7, 16, 29].

First, we assume that the operators F_i are continuously Fréchet differentiable, and also that there exist $x_0 \in X$, $M > 0$, and $\rho > 0$ such that

$$\|F'_i(x)\| \leq M, \quad x \in B_\rho(x_0) \subset \bigcap_{i=0}^{N-1} D_i. \quad (10)$$

Notice that $x_0^\delta = x_0$ is used as starting value of the L-SDK iteration. Next we make an uniform assumption on the nonlinearity of the operators F_i . Namely, we assume that the *local tangential cone condition* [7, 16]

$$\begin{aligned} \|F_i(x) - F_i(\bar{x}) - F'_i(x)(x - \bar{x})\|_Y \\ \leq \eta \|F_i(x) - F_i(\bar{x})\|_Y, \quad x, \bar{x} \in B_\rho(x_0) \end{aligned} \quad (11)$$

holds for some $\eta < 1/2$. Moreover, we assume the existence of an element

$$x^* \in B_{\rho/2}(x_0) \text{ such that } F(x^*) = y. \quad (12)$$

where $y = (y^0, \dots, y^{N-1})$ is the exact data satisfying (1).

We are now in position to choose the positive constants α_{\min} , τ in (7), (6). For the rest of this article we shall assume

$$\alpha_{\min} \geq \Phi_{\text{rel}}(1/M^2), \quad (13)$$

$$\tau \geq 2 \frac{1 + \eta}{1 - 2\eta} \geq 2. \quad (14)$$

In particular, for linear problems we can choose τ equal to 2.

In the sequel we verify some basic results that are necessary for the convergence analysis derived in the next section. The first result concerns the well-definedness and positivity of the relaxation parameter α_k .

Lemma 2.1. *Let assumptions (10)-(12) be satisfied. Then the coefficients α_k in (7) are well-defined and positive.*

Proof. If $\omega_k = 0$, the assertion follows from (7). If $\omega_k = 1$, then $\|F_{[k]}(x_k^\delta) - y_{[k]}^\delta\| \geq \tau\delta_{[k]}$ and the assertion is a consequence of [29, Lemma 3.1], applied to $F_{[k]}$ instead of F . \square

In the next lemma we prove an estimate for the step size of the L-SDK iteration.

Lemma 2.2. *Let s_k and α_k be defined by (5) and (7). Then*

$$\alpha_k \|s_k\|^2 \leq \|F_{[k]}(x_k^\delta) - y_{[k]}^\delta\|^2, \quad k \in \mathbb{N}. \quad (15)$$

Proof. It is enough to consider the case $\omega_k = 1$. It follows from (7) that

$$\alpha_k \|s_k\|^2 = \Phi_{\text{rel}} \left(\frac{\|s_k\|^2}{\|F'_{[k]}(x_k^\delta) s_k\|^2} \right) \|s_k\|^2 \leq \frac{\|s_k\|^4}{\|F'_{[k]}(x_k^\delta) s_k\|^2}. \quad (16)$$

Moreover, from the definition of s_k we obtain

$$\begin{aligned} \|F'_{[k]}(x_k^\delta) s_k\| &= \|F'_{[k]}(x_k^\delta) F'_{[k]}(x_k^\delta)^* [F_{[k]}(x_k^\delta) - y_{[k]}^\delta]\|, \\ \|s_k\|^2 &\leq \|F'_{[k]}(x_k^\delta) F'_{[k]}(x_k^\delta)^* [F_{[k]}(x_k^\delta) - y_{[k]}^\delta]\| \|F_{[k]}(x_k^\delta) - y_{[k]}^\delta\|. \end{aligned}$$

Now, substituting the last two expressions in (16), shows (15). \square

The following Lemma is an important auxiliary result, which will be used at several places throughout the article.

Lemma 2.3. *Let x_k^δ , α_k , ω_k , and s_k be defined by (4) - (7) and assume that (11), (12) hold true. If $x_k^\delta \in B_{\rho/2}(x^*)$ for some $k \geq 0$, then*

$$\begin{aligned} \|x_{k+1}^\delta - x^*\|^2 - \|x_k^\delta - x^*\|^2 & \\ \leq \omega_k \alpha_k \|F_{[k]}(x_k^\delta) - y_{[k]}^\delta\| & \left((2\eta - 1) \|F_{[k]}(x_k^\delta) - y_{[k]}^\delta\| + 2(1 + \eta)\delta_{[k]} \right). \end{aligned} \quad (17)$$

Proof. If $\omega_k = 0$, then $x_{k+1} = x_k$ and (17) follows with equality. If $\omega_k \neq 0$, it follows from (4) and (5) and Lemma 2.2 that

$$\begin{aligned}
& \|x_{k+1}^\delta - x^*\|^2 - \|x_k^\delta - x^*\|^2 \\
&= 2\langle x_k^\delta - x^*, x_{k+1}^\delta - x_k^\delta \rangle + \|x_{k+1}^\delta - x_k^\delta\|^2 \\
&= 2\omega_k \alpha_k \langle x_k^\delta - x^*, F'_{[k]}(x_k^\delta)^*(y_{[k]}^\delta - F_{[k]}(x_k^\delta)) \rangle + (\alpha_k \omega_k)^2 \|s_k\|^2 \\
&\leq 2\omega_k \alpha_k \langle y_{[k]}^\delta - F_{[k]}(x_k^\delta), F'_{[k]}(x_k^\delta)(x_k^\delta - x^*) \rangle + \omega_k \alpha_k \|F_{[k]}(x_k^\delta) - y_{[k]}^\delta\|^2 \\
&\leq \omega_k \alpha_k \left(2\langle y_{[k]}^\delta - F_{[k]}(x_k^\delta), F'_{[k]}(x_k^\delta)(x^* - x_k^\delta) - F_{[k]}(x^*) + F_{[k]}(x_k^\delta) \rangle \right. \\
&\quad \left. + 2\langle y_{[k]}^\delta - F_{[k]}(x_k^\delta), y_{[k]} - y_{[k]}^\delta \rangle - \|y_{[k]}^\delta - F_{[k]}(x_k^\delta)\|^2 \right).
\end{aligned}$$

Now, applying (11) with $x = x^*$ and $\bar{x} = x_k^\delta \in B_{\rho/2}(x^*) \subset B_\rho(x_0)$, leads to

$$\begin{aligned}
& \|x_{k+1}^\delta - x^*\|^2 - \|x_k^\delta - x^*\|^2 \\
&\leq \omega_k \alpha_k \|F_{[k]}(x_k^\delta) - y_{[k]}^\delta\| \left(2\eta \|F_{[k]}(x_k^\delta) - y_{[k]}\| + 2\delta_{[k]} - \|F_{[k]}(x_k^\delta) - y_{[k]}^\delta\| \right).
\end{aligned}$$

The last inequality and (1) show (17). \square

Our next goal is to prove a monotony property, known to be satisfied by other iterative regularization methods, e.g., by the Landweber [7], the steepest descent [29], the LK [17], and the L-LK [11] method.

Proposition 2.4 (Monotonicity). *Under the assumptions of Lemma 2.3,*

$$\|x_{k+1}^\delta - x^*\|^2 \leq \|x_k^\delta - x^*\|^2, \quad k \in \mathbb{N}. \quad (18)$$

Moreover, all iterates x_k^δ remain in $B_{\rho/2}(x^*) \subset B_\rho(x_0)$ and satisfy (17).

Proof. From (12) it follows that $x_0 \in B_{\rho/2}(x^*)$. If $\omega_0^\delta = 0$, then x_1 satisfies (18) with equality and $x_1 \in B_{\rho/2}(x^*) \subset B_\rho(x_0)$. If $\omega_0^\delta \neq 0$, then Lemma 2.3 implies

$$\begin{aligned}
\|x_1^\delta - x^*\|^2 - \|x_0^\delta - x^*\|^2 &\geq (2\eta - 1) \|F_0(x_0^\delta) - y^{\delta,0}\| + 2(1 + \eta)\delta^0 \\
&\geq \delta^0 \left((2\eta - 1)\tau + 2(1 + \eta) \right) \geq 0.
\end{aligned}$$

Therefore (18), for $k = 0$, follows from (14). In particular, $x_1 \in B_{\rho/2}(x^*)$. An inductive argument implies (18) and that $x_k \in B_{\rho/2}(x^*) \subset B_\rho(x_0)$ for all $k \in \mathbb{N}$. The assertions therefore follows from Lemma 2.3. \square

3 Convergence Analysis of the Loping Steepest Descent Kaczmarz Method

In this section we provide a complete convergence analysis for the L-SDK iteration, showing that it is a convergent regularization method in the sense

of [7] (see Theorems 3.3 and 3.6 below). Throughout this section, we assume that (10) - (12) hold, and that x_k^δ , α_k , ω_k , and s_k are defined by (4) - (7).

Our first goal is to prove convergence of the L-SDK iteration for $\delta = 0$. For exact data $y = (y_0, \dots, y_{N-1})$, the iterates in (4) are denoted by x_k .¹

Lemma 3.1. *There exists a x_0 -minimal norm solution x^\dagger of (2) in $B_{\rho/2}(x_0)$, i.e., a solution x^\dagger of (2) such that*

$$\|x^\dagger - x_0\| = \inf \{ \|x - x_0\| : x \in B_{\rho/2}(x_0) \text{ and } F(x) = y \}.$$

Moreover, x^\dagger is the only solution of (2) in $B_{\rho/2}(x_0) \cap (x_0 + \ker(F'(x^\dagger)))^\perp$.

Proof. Lemma 3.1 is a consequence of [13, Proposition 2.1]. A detailed proof can be found in [16]. \square

Lemma 3.2. *For all $k \in \mathbb{N}$, we have $\alpha_k \geq \underline{\alpha}$.*

Proof. For the $\omega_k = 0$ the claimed estimate holds with equality. If $\omega_k = 1$, it follows from (10) that

$$\|s_k\|^2 / \|F'_{[k]}(x_k^\delta) s_k\|^2 \geq \|F'_{[k]}(x_k^\delta)\|^{-2} \geq 1/M^2.$$

Now the monotonicity of Φ_{rel} implies $\alpha_k \geq \Phi_{\text{rel}}(M^{-2}) = \alpha_{\min}$. \square

Throughout the rest of this article, x^\dagger denotes the x_0 -minimal norm solution of (2). We define $e_k := x^\dagger - x_k$. From Proposition 2.4 it follows that (17) holds for all k . By adding over all k , this leads

$$\sum_{i=0}^{\infty} \alpha_i \|y_{[i]} - F_{[i]}(x_i)\|^2 \leq \frac{\|x_0 - x^\dagger\|}{1 - 2\eta} < \infty. \quad (19)$$

Equation (19) and the monotony of $\|e_k\|$ shown in Proposition 2.4 are main ingredients in the following proof of the convergence of the SDK iteration.

Theorem 3.3 (Convergence for Exact Data). *For exact data, the iteration (x_k) converges to a solution of (2), as $k \rightarrow \infty$. Moreover, if*

$$\mathcal{N}(F'(x^\dagger)) \subseteq \mathcal{N}(F(x)) \text{ for all } x \in B_\rho(x_0), \quad (20)$$

then $x_k \rightarrow x^\dagger$.

Proof. From (18) it follows that $\|e_k\|$ decreases monotonically and therefore that $\|e_k\|$ converges to some $a \geq 0$. In the following we show that e_k is in fact a Cauchy sequence.

¹This is a standard notation used in the literature.

For $k = k_0N + k_1$ and $l = l_0N + l_1$ with $k \leq l$ and $k_1, l_1 \in \{0, \dots, N-1\}$, let $n_0 \in \{k_0, \dots, l_0\}$ be such that

$$\sum_{i_1=0}^{N-1} \|F_{i_1}(x_{Nn_0+i_1}) - y_{i_1}\| \leq \sum_{n_1=0}^{N-1} \|F_{i_1}(x_{Ni_0+i_1}) - y_{i_1}\|, \quad i_0 \in \{k_0, \dots, l_0\}. \quad (21)$$

Then, with $n := Nn_0 + N - 1$, we have

$$\|e_k - e_l\| \leq \|e_k - e_n\| + \|e_l - e_n\| \quad (22)$$

and

$$\begin{aligned} \|e_n - e_k\|^2 &= \|e_k\|^2 - \|e_n\|^2 + 2\langle e_n - e_k, e_n \rangle^2, \\ \|e_n - e_l\|^2 &= \|e_l\|^2 - \|e_n\|^2 + 2\langle e_n - e_l, e_n \rangle^2, \end{aligned} \quad (23)$$

For $k \rightarrow \infty$, the first two terms of (23) converge to $\epsilon - \epsilon = 0$. Therefore, in order to show that e_k is a Cauchy sequence, it is sufficient to prove that $\langle e_n - e_k, e_n \rangle$ and $\langle e_n - e_l, e_n \rangle$ converge to zero as $k \rightarrow \infty$.

To that end, we write $i = Ni_0 + i_1$, $i_1 \in \{0, \dots, N-1\}$ and set $i^* := Nn_0 + i_1$. Then, using the definition of the steepest descent Kaczmarz iteration it follows that

$$\begin{aligned} &|\langle e_n - e_k, e_n \rangle| \\ &= \left| \sum_{i=k}^{n-1} \alpha_i \langle F'_{i_1}(x_i)^* (y^{i_1} - F_{i_1}(x_i)), x^\dagger - x_n \rangle \right| \\ &\leq \sum_{i=k}^{n-1} \alpha_i \left| \langle y^{i_1} - F_{i_1}(x_i), F'_{i_1}(x_i)(x^\dagger - x_{i^*}) + F'_{i_1}(x_i)(x_{i^*} - x_n) \rangle \right| \\ &\leq \sum_{i=k}^{l-1} \alpha_i \|y^{i_1} - F_{i_1}(x_i)\| \|F'_{i_1}(x_i)(x^\dagger - x_{i^*})\| \\ &\quad + \sum_{i=k}^{l-1} \alpha_i \|y^{i_1} - F_{i_1}(x_i)\| \|F'_{i_1}(x_i)(x_{i^*} - x_n)\| \end{aligned} \quad (24)$$

From (11) it follows immediately that

$$\|F'_{i_1}(x_i)(x^\dagger - x_{i^*})\| \leq (1 + \eta) \|y^{i_1} - F_{i_1}(x_{i^*})\|. \quad (25)$$

Again using the definition of the steepest descent Kaczmarz iteration and equations (7), (10), it follows that

$$\begin{aligned} &\|F'_{i_1}(x_i)(x_{i^*} - x_n)\| \leq M \|x_{i^*} - x_n\| \\ &\leq M \sum_{j=i_1}^{N-2} \alpha_j \|F'_j(x_{Nl_0+j})^* (F_j(x_{Nn_0+j}) - y^j)\| \\ &\leq \alpha_{\max} M^2 \sum_{j=i_1}^{N-2} \|F_j(x_{Nn_0+j}) - y^j\| \leq \sum_{j=0}^{N-1} \|F_j(x_{Nn_0+j}) - y^j\| \end{aligned} \quad (26)$$

where, for the last estimate we used that $\alpha_{\max}M^2 = \Phi_{\text{rel}}(\alpha_{\max})M^2 \leq 1$. Substituting (25), (26) in (24) leads to

$$\begin{aligned} & |\langle e_n - e_k, e_n \rangle| \\ & \leq (2 + \eta) \sum_{i_0=k_0}^{n-1} \sum_{i_1=0}^{N-1} \alpha_i \|y^{i_1} - F_{i_1}(x_{Ni_0+i_1})\| \left(\sum_{j=0}^{N-1} \|F_j(x_{Nn_0+j}) - y_j\| \right) \\ & \leq (2 + \eta) \alpha_{\max} \sum_{i_0=k_0}^{n-1} \left(\sum_{i_1=0}^{N-1} \|y^{i_1} - F_{i_1}(x_{Ni_0+i_1})\| \right)^2 \end{aligned}$$

So we finally obtain the estimate

$$|\langle e_n - e_k, e_n \rangle| \leq \frac{N(2 + \eta)\alpha_{\max}}{\alpha_{\min}} \sum_{i_0=k_0}^{n-1} \sum_{i_1=0}^{N-1} \alpha_{Ni_0+i_1} \|y^{i_1} - F_{i_1}(x_{Ni_0+i_1})\|^2.$$

Because of (19), the last sum tends to infinity for $k = Nk_0 + k_1 \rightarrow \infty$, and therefore $\langle e_n, e_n - e_k \rangle \rightarrow 0$. Analogously one shows that $\langle e_n, e_n - e_l \rangle \rightarrow 0$. Therefore e_k is a Cauchy sequence and $x_k = x^\dagger - e_k$ converges to an element $x^* \in X$. Because all residuals $\|F_{[k]}(x_k) - y_{[k]}\|$ tend to zero, x^* is solution of (2).

Now assume $\mathcal{N}(F'(x^\dagger)) \subseteq \mathcal{N}(F(x))$, for $x \in B_\rho(x_0)$. Then from the definition of x_k it follows that

$$x_{k+1} - x_k \in \mathcal{R}(F'_{[k]}(x_k)) \subset \mathcal{R}(F'(x_k)) \subset \mathcal{N}(F'(x_k))^\perp \subset \mathcal{N}(F'(x^\dagger))^\perp.$$

An inductive argument shows that all iterates x_k are elements of $x_0 + \mathcal{N}(F'(x^\dagger))^\perp$. Together with the continuity of $F'(x^\dagger)$ this implies that $x^* \in x_0 + \mathcal{N}(F'(x^\dagger))^\perp$. By Lemma 3.1, x^\dagger is the only solution of (2) in $B_{\rho/2}(x_0) \cap (x_0 + \mathcal{N}(F'(x^\dagger))^\perp)$, and so the second assertion follows. \square

The second goal in this section is to prove that $x_{k_*}^\delta$ converges to a solution of (2), as $\delta \rightarrow 0$. First we verify that, for noisy data, the stopping index k_*^δ defined in (8) is finite.

Proposition 3.4 (Stopping Index). *Assume $\delta_{\min} := \min\{\delta_0, \dots, \delta_{N-1}\} > 0$. Then k_*^δ defined in (8) is finite, and*

$$\|F_i(x_{k_*^\delta}^\delta) - y_i^\delta\| \leq \tau \delta^i, \quad i = 0, \dots, N-1. \quad (27)$$

Proof. Assume that for every $l \in \mathbb{N}$, there exists $i(l) \in \{0, \dots, N-1\}$ such that $x_{lN+i(l)} \neq x_{lN}$. From Proposition 2.4 follows that we can apply (17) recursively for $k = 1, \dots, lN$ and obtain

$$\begin{aligned} -\|x_0 - x^*\|^2 & \leq \sum_{k=1}^{lN} \omega_k \alpha_k \delta_{[k]} \|F_{[k]}(x_k^\delta) - y_{[k]}^\delta\| \\ & \left(2(1 + \eta)\delta_{[k]} - (1 - 2\eta)\|F_{[k]}(x_k^\delta) - y_{[k]}^\delta\| \right), \quad l \in \mathbb{N}. \end{aligned}$$

Using the fact that, either $\omega_k = 0$ or $\|F_{[k]}(x_k^\delta) - y_{[k]}^\delta\| > \tau\delta^k$, implies

$$\|x_0 - x^*\|^2 \geq \left(\tau(1 - 2\eta) - 2(1 + \eta)\right) \sum_{k=1}^{lN} \alpha_k \delta_{[k]} \|F_{[k]}(x_k^\delta) - y_{[k]}^\delta\|. \quad (28)$$

Equation (28) and Lemma 3.2 imply

$$\|x_0 - x^*\|^2 > \left(\tau(1 - 2\eta) - 2(1 + \eta)\right) \underline{\alpha} \delta_{\min} l, \quad l \in \mathbb{N}. \quad (29)$$

The right hand side in (29) tends to infinity, which gives a contradiction. Consequently, $\{l \in \mathbb{N} : x_{lN+i} = x_{lN}, 0 \leq i \leq N - 1\} \neq \emptyset$ and the infimum in (8) takes a finite value.

To prove (27), assume to the contrary, that $\|F_i(x_{k_\delta}^\delta) - y_i^\delta\| > \tau\delta^i$ for some $i \in \{0, \dots, N - 1\}$. From (6) and (8) it follows that, $\omega_k = 1$ and $x_{k_\delta^*+i}^\delta = x_{k_\delta^*+i+1}^\delta$ respectively. Thus, Proposition 2.4 and Lemma 2.1 imply

$$0 \leq (2\eta - 1) \|F_i(x_{k_\delta^*}^\delta) - y_i^\delta\| + 2(1 + \eta)\delta^i < \delta^i \left((2\eta - 1)\tau + 2(1 + \eta) \right).$$

This contradicts (14), concluding the proof of (27). \square

The last auxiliary result concerns the continuity of x_k^δ at $\delta = 0$. For $y, y^\delta \in Y^N$, $\delta > 0$, and $k \in \mathbb{N}$ we define

$$\Delta_k(\delta, y, y^\delta) := \omega_k F'_{[k]}(x_k^\delta)^* (F_{[k]}(x_k^\delta) - y_{[k]}^\delta) - F'_{[k]}(x_k)^* (F_{[k]}(x_k) - y_{[k]}).$$

Lemma 3.5. For all $k \in \mathbb{N}$,

$$\limsup_{\delta \rightarrow 0} \left\{ \|\Delta_k(\delta, y, y^\delta)\| : y^\delta \in Y^N, \|y_i - y_i^\delta\| \leq \delta_i \right\} = 0. \quad (30)$$

Moreover, $x_{k+1}^\delta \rightarrow x_{k+1}$, as $\delta \rightarrow 0$.

Proof. We prove Lemma 3.5 by induction. The case $k = 0$ is similar to the case general case and is omitted.

Now, assume $k > 0$ and that (30) holds for all $k' < k$. First we note that (30) and the continuity of Φ_{rel} obviously imply $x_{k+1}^\delta \rightarrow x_{k+1}$, as $\delta \rightarrow 0$ because. For the proof of (30) we consider two cases. In the first case, $\omega_k = 1$, we have

$$\|\Delta_k(\delta, y, y^\delta)\| = \|F'_{[k]}(x_k^\delta)^* (F_{[k]}(x_k^\delta) - y_{[k]}^\delta) - F'_{[k]}(x_k)^* (F_{[k]}(x_k) - y_{[k]})\|$$

In the second case $\omega_k = 0$ we have $\|F_{[k]}(x_k^\delta) - y_{[k]}^\delta\| \leq \tau\delta^k$ and consequently

$$\begin{aligned} \|\Delta_k(\delta, y, y^\delta)\| &\leq \|F'_{[k]}(x_k)^* (F_{[k]}(x_k) - y_{[k]})\| \\ &\leq \|F'_{[k]}(x_k^\delta)\| \left(\|F_{[k]}(x_k) - F_{[k]}(x_k^\delta)\| + \|F_{[k]}(x_k^\delta) - y_{[k]}^\delta\| + \|y_{[k]}^\delta - y_{[k]}\| \right) \\ &\leq \|F'_{[k]}(x_k^\delta)\| \left(\|F_{[k]}(x_k) - F_{[k]}(x_k^\delta)\| + (\tau + 1) \delta_{[k]} \right). \end{aligned}$$

Now (30) follows from (10), the continuity of $F_{[k]}$ and $F'_{[k]}$, and the induction hypothesis (which implies $x_k^\delta \rightarrow x_k$). \square

Theorem 3.6 (Convergence for Noisy Data). *Assume $(\delta_j^0, \dots, \delta_j^{N-1})$ is a sequence in $(0, \infty)^N$ with $\lim_{j \rightarrow \infty} \delta_i^j = 0$, for $j \in \mathbb{N}$. Let $(y_0^j, \dots, y_{N-1}^j)$ be a sequence of noisy data satisfying*

$$\|y_i^j - y_i\| \leq \delta_i^j, \quad i = 0, \dots, N-1, j \in \mathbb{N},$$

and let $k^j := k_*(\delta^j, y^{\delta^j})$ denote the corresponding stopping index defined in (8). Then $x_{k^j}^{\delta^j}$ converges to a solution of (2), as $j \rightarrow \infty$. Moreover, if (20) holds, then $x_{k^j}^{\delta^j} \rightarrow x^\dagger$.

Proof. Let x^* denote the limit of the iterates x_k which is a solution of (2), cf. Theorem 3.3. From Lemma 3.5 and the continuity of F_i we know that, for any fixed $k \in \mathbb{N}$,

$$x_k^{\delta^j} \rightarrow x_k, \quad F_i(x_k^{\delta^j}) \rightarrow F_i(x_k), \quad \text{as } j \rightarrow \infty. \quad (31)$$

To show that $x_{k^j}^{\delta^j} \rightarrow x^*$, we first assume that k^j has a finite accumulation point k_* . Without loss of generality we may assume that $k^j = k_*$ for all $j \in \mathbb{N}$. From Proposition 3.4 we now that $\|y_i^{\delta^j} - F_i(x_{k_*}^{\delta^j})\| < \tau \delta^i$ and, by taking the limit $j \rightarrow \infty$, that $y^i = F_i(x_{k_*})$. Consequently $x_{k_*} = x^*$ and $x_{k_*}^j \rightarrow x^*$ as $j \rightarrow \infty$.

It remains to consider the case where $k^j \rightarrow \infty$ as $j \rightarrow \infty$. To that end let $\varepsilon > 0$. Without loss of generality we assume that k^j is monotonically increasing. According to Theorem 3.3 we can choose $n \in \mathbb{N}$ such that $\|x_{k^n} - x^*\| < \varepsilon/2$. Equation (31) implies that there exists $j_0 > n$ such that $\|x_{k^n}^{\delta^j} - x_{k^n}\|$ for all $j \geq j_0$. This and Proposition 2.4 imply

$$\begin{aligned} \|x_{k^j}^{\delta^j} - x^*\| &\leq \|x_{k^n}^{\delta^j} - x^*\| \\ &\leq \|x_{k^n}^{\delta^j} - x_{k^n}\| + \|x_{k^n} - x^*\| < \frac{\varepsilon}{2} + \frac{\varepsilon}{2} = \varepsilon, \quad \text{for } j \geq j_0. \end{aligned}$$

Consequently, $x_{k^j}^{\delta^j} \rightarrow x^*$.

If (20) holds true, then by Theorem 3.3 $x^* = x^\dagger$. Therefore $x_{k^j}^{\delta^j} \rightarrow x^\dagger$, which concludes the proof. \square

Remark 3.7. *In standard iterative regularization methods the number of performed iterations plays the role of the regularization parameter [7, 16]. A parameter choice rule corresponds to the choice of an appropriate stopping index $k_*^\delta = k(\delta, y^\delta)$.*

For the loping Kaczmarz iterations analyzed in this article, the situation is quite different. If k is fixed, then the iterates x_k^δ , do not depend continuously on data y_i^δ . However, for a fixed sequence (ω_k) of loping parameters, the iterates x_k^δ do depend continuously on y_i^δ : Now, the loping sequences (ω_k) play the role of the regularization parameters and the particular sequence $\omega_k = \omega_k(\delta, y^\delta)$, depending on δ_i and the noisy data y_i^δ , is the a-posteriori parameter choice rule.

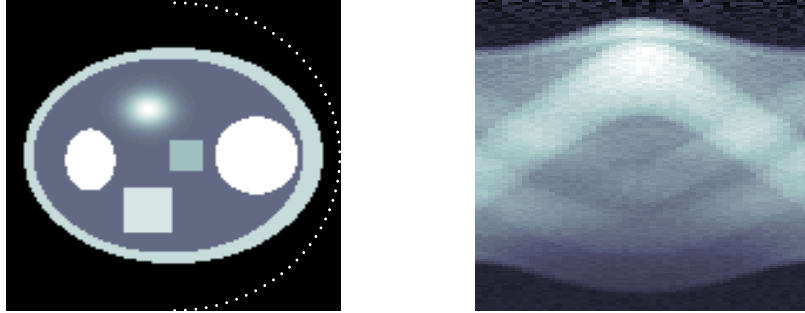


Figure 2: The left picture shows the phantom x^\dagger , where the white dots indicate the locations of the detectors. The corresponding data $(y_i^\delta)_i$ are depicted on the right.

4 Limited View Problem in Photoacoustic Computed Tomography

In this section we compare the numerical performance of loping Kaczmarz methods applied to a system of linear equations related to a limited view problem in *photoacoustic computed tomography* [8, 18, 28, 34].

Let $X := L^2(D)$ denote the Hilbert space of all square integrable functions in the unit disc $D \subset \mathbb{R}^2$, and let Y denote the Hilbert space of all functions $y : [0, 2] \rightarrow \mathbb{R}$ with $\|y\| := \int_0^2 y(t)tdt < \infty$. We consider the system

$$\mathbf{M}_i x = y_i, \quad i = 0, \dots, N - 1, \quad (32)$$

where $\mathbf{M}_i : X \rightarrow Y$,

$$(\mathbf{M}_i x)(t) := \frac{1}{\sqrt{\pi}} \int_{S^1} x(\xi_i + t\sigma) d\Omega(\sigma), \quad t \in [0, 2], \quad (33)$$

are scaled versions of *circular mean Radon transform*. Solving (32) is the crucial step in three-dimensional photoacoustic computed tomography with integrating linear detectors [9, 28], where the centers of integration, ξ_i , correspond to the positions of the linear detectors. The operators \mathbf{M}_i are linear, bounded, and satisfy $\|\mathbf{M}_i\| \leq 1$, [10]. For linear bounded operators, the *tangential cone condition* (11) is satisfied with $\eta = 0$. Consequently, the L-SDK method (4) - (7) provides a convergent regularization method for solving (32). The adjoint of \mathbf{M}_i , required in (5) is given by $(\mathbf{M}_i^* y)(\xi) = y(|\xi_i - \xi|)/\sqrt{\pi}$, [10].

In the following numerical examples, we consider the L-SDK method with either the choice $\Phi_{\text{rel}}(s) = \alpha_{\min}s$ (which minimizes $\|F_{[k]}(x_{k+1}^\delta) - y_{[k]}^\delta\|^2$) or $\Phi_{\text{rel}}(s) = \alpha_{\min}$ (which corresponds to the L-LLK method). In both cases

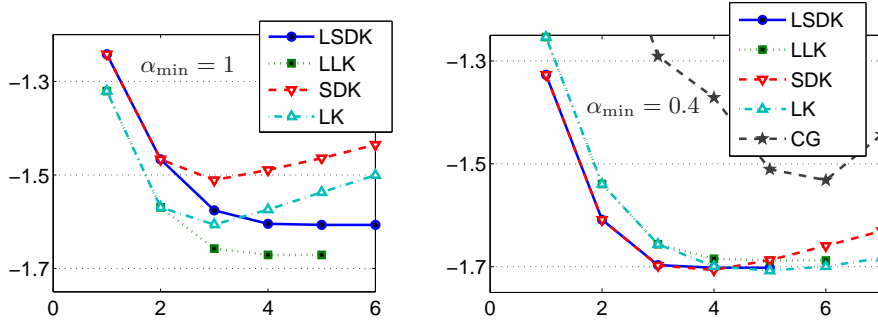


Figure 3: Evolution of the relative error $\ln \|x^\dagger - x_k^\delta\|/\|x^\dagger\|$ for $\alpha_{\min} = 1$ (left) and $\alpha_{\min} = 0.4$ (right).

we use $\alpha_{\min} = 0.4$ or $\alpha_{\min} = 1$. We will assume $N = 50$ measurements, where the centers $\xi_i = R(\sin(\pi i/(N-1)) \cos(\pi i/(N-1)))$ are uniformly distributed on the semicircle $S^+ := \{(\xi^1, \xi^2) \in \partial B_R : \xi_1 \geq 0\}$. Micro-local analysis predicts, that in such a limited angle situation where the centers do not cover the hole circle, certain details (the *invisible* boundaries) of x outside the detection region (convex hull of S^+) cannot be recovered [21, 27, 35]. The phantom x^\dagger , shown in the left picture in Figure 2, consists of a superposition of characteristic functions and one Gaussian kernel. Data $y_i = \mathbf{M}_i x^\dagger$ was calculated via numerical integration with the trapezoidal rule and 4% noise was added, such that $\|y_i - y_i^\delta\|/\|y_i\| \approx 0.04$.

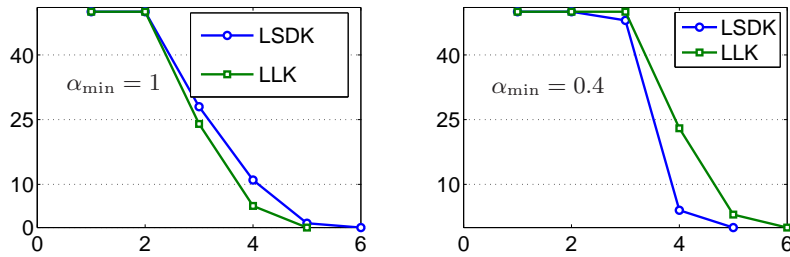


Figure 4: Actually performed number of iterations within a cycle for $\alpha_{\min} = 1$ (left) and $\alpha_{\min} = 0.4$ (right).

Figures 3 and 4 show the reconstruction error $e_k^\delta := \|x_k^\delta - x^\dagger\|$ and the number of actually performed iterations respectively. For comparison purposes, the error for the SDK and the LK iteration (without loping parameter) are plotted. The smaller relaxation parameter ω_{\min} gives smaller reconstruction errors. This behavior is typically for the application of Kaczmarz type iterations to Radon transforms [5, 24]; therefore in praxis often

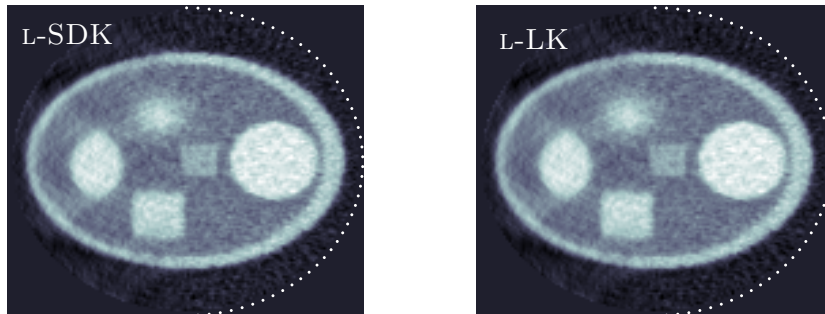


Figure 5: Numerical reconstruction of the phantom depicted in Figure 2 with $\alpha_{\min} = 0.4$. Left: result of L-SDK method. Right: result of L-LK method.

relatively small relaxation parameters are chosen. As can be seen in Figure 3, for the larger relaxation parameter, the loping strategy significantly reduces the reconstruction error. For the smaller relaxation parameter, the regularized solution of the loping Kaczmarz methods have errors comparable to the optimal solution of their non-loping counterparts when stopped after the cycle with minimal error (which is not available in practice). In Figure 5 the regularized solutions are depicted with $\alpha_{\min} = 0.4$.

	Cycles	Runtime (sec)	Error (%)
L-SDK	5	21.9	18.2
L-LK	6	21.4	18.5
SDK	4	24.5	18.2
LK	5	16.9	18.1
CGNE	5	38.2	21.6

Table 1: Numerical performance of Kaczmarz methods for $\hat{\alpha} = 0.4$, and the CGNE method. The non-loping iterations are stopped after the cycle when the error $\|x_k^\delta - x^\dagger\|$ is minimal.

To point out the effectiveness of the loping Kaczmarz methods for solving linear inconsistent systems we included the reconstruction error for the CGNE iteration (conjugate gradient [14, 31] applied to normal equations). If stopped appropriately the CGNE method is known to be a regularization method [7, 12]. As can be seen in Figure 3 the error for the L-SDK and the L-LK methods much smaller than for the CGNE iteration. In Table 1 run times on a 2 GHz Intel Core Duo iMac are compared. The image is reconstructed on a 120×120 grid.

5 An inverse doping problem

In this section we present another comparison of the numerical performance of the L-SDK, L-LK and LK methods. This time we consider an application related to *inverse doping problems* for semiconductors [2, 10, 20, 3] For details on the mathematical modeling of this inverse problem we refer the reader to [10, Section 3].

In what follows we describe the abstract formulation in Hilbert spaces of the problem (the so called *inverse doping problem in the linearized unipolar model for current flow measurements*). Let $\Omega = (0, 1) \times (0, 1) \subset \mathbb{R}^2$ be the domain representing the semiconductor device (a diode). The two semiconductor contacts are represented by the boundary parts:

$$\Gamma_0 := \{(s, 0) : s \in (0, 1)\}, \quad \Gamma_1 := \{(s, 1) : s \in (0, 1)\},$$

(we denote $\partial\Omega_D := \Gamma_0 \cup \Gamma_1$) while the insulated surfaces of the semiconductor are represented by $\partial\Omega_N := \{(0, t) : t \in (0, 1)\} \cup \{(1, t) : t \in (0, 1)\}$. This specific inverse doping problem can be reduced to the identification of the positive parameter function x (the doping profile C is related to x by $C = x - \lambda^2 \Delta(\ln x)$) in the model

$$\mu_n \nabla \cdot (x(\xi) \nabla u) = 0, \quad \text{in } \Omega \quad (34)$$

$$u = U(\xi), \quad \text{on } \partial\Omega_D \quad (35)$$

$$\nabla u \cdot \nu = 0, \quad \text{on } \partial\Omega_N \quad (36)$$

from measurements of the Voltage–Current map (the forward operator)

$$\begin{aligned} \Sigma_x : H^{3/2}(\partial\Omega_D) &\rightarrow \mathbb{R}, \\ U &\mapsto \mu_n \int_{\Gamma_1} e^{V_{\text{bi}}(\xi)} u_\nu(\xi) d\Gamma \end{aligned}$$

which maps an applied potential U at $\partial\Omega_D$ to the corresponding *total current flow* $\Sigma_x(U)$ through the contact Γ_1 . Here μ_n, λ are positive constants and V_{bi} is a known logarithmic function defined on $\partial\Omega_D$.

Due to the nature of the practical experiments that can be performed on a factory environment, some restrictions on the data have to be taken into account:

1. The voltage profiles $U \in H^{3/2}(\partial\Omega_D)$ must satisfy $U(\xi) \equiv 0$ at the contact Γ_1 .
2. The parameter x has to be determined from a finite number of measurements, i.e. from the data

$$y_i^\delta := \Sigma_x(U_i) \in Y := \mathbb{R}, \quad i = 0, \dots, N-1, \quad (37)$$

where the $U_i \in H^{3/2}(\partial\Omega_D)$ are prescribed voltage profiles satisfying 1.

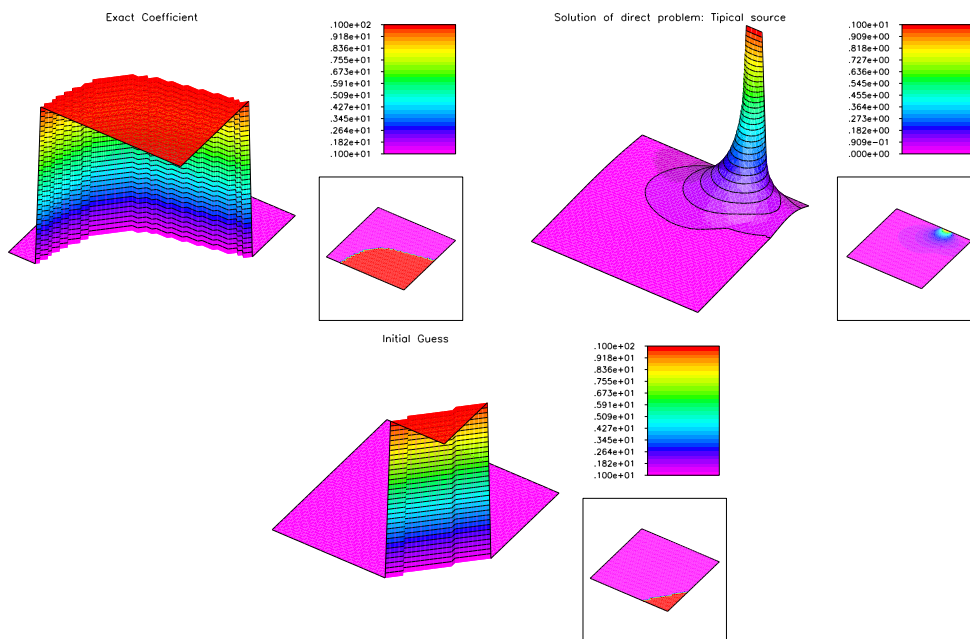


Figure 6: In the top left picture, the doping profile to be identified. In the top right picture, a typical voltage profile U_i and the corresponding solution u of (34)–(36). The initial guess used for the L-SDK, L-LK and LK iterative methods is shown in the bottom picture. The boundary parts Γ_0 and Γ_1 correspond to the top right and to the lower left edge respectively (the origin is the right corner).

Therefore we can model the inverse doping problem with a system of operator equations of the form (2), namely

$$F_i(x) = y_i^\delta, \quad i = 0, \dots, N-1,$$

where $x \in L^2(\Omega) =: X$ is the unknown parameter, $y_i^\delta \in \mathbb{R} =: Y$ denote the measured data, $F_i : X \rightarrow Y$ defined by $F_i(x) := \Sigma_x(U_i)$ are the parameter to output maps, with domains of definition

$$D_i := \{x \in L^\infty(\Omega) : 0 < x_{\min} \leq x \leq x_{\max}, \text{ a.e.}\}.$$

It is worth mentioning that, although the operators F_i are Fréchet differentiable, they do not satisfy the tangential cone condition (11). Therefore, the convergence results derived in Section 3 cannot be applied.

In the following numerical examples we assume that $N = 11$ Dirichlet–Neumann pairs $(U_i, F_i(x'))$ of measurement data are available. The fixed inputs U_i , are chosen to be piecewise constant functions supported in Γ_0

$$U_i(s) := \begin{cases} 1, & |s - s_i| \leq h \\ 0, & \text{else} \end{cases}$$

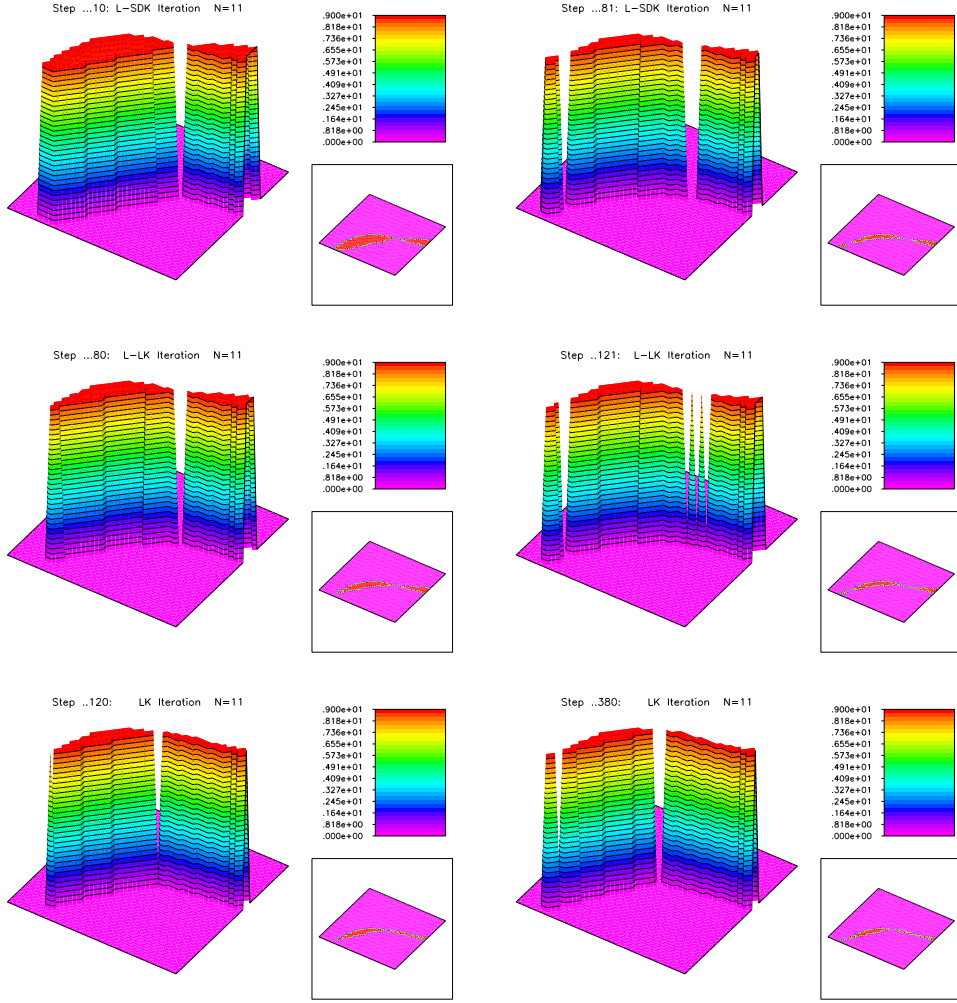


Figure 7: Comparison between the L-SDK, L-LK and LK methods. The top two pictures show the results obtained by the L-SDK iteration after 10 and 81 cycles. The two central pictures show the results obtained by the L-LK iteration after 80 and 121 cycles. The two bottom pictures show the results obtained by the LK after 120 and 380 cycles.

where the points s_i are uniformly distributed on Γ_0 and $h = 1/32$. The doping profile to be reconstructed is shown in Figure 6 (top left picture). The top right picture of Figure 6 shows a typical voltage profile U_j (applied at Γ_0) as well as the corresponding solution u of (34)–(36). In these pictures, as well as in the forthcoming ones, Γ_1 appears on the lower left edge and Γ_0 on the top right edge (the origin corresponds to the upper right corner).

In Figure 7 we show the evolution of the iteration error for the L-SDK, L-LK and LK methods. The same initial guess was used for the three methods (see Figure 6). In our computations we chose $\tau = 2.5$ in (14). The

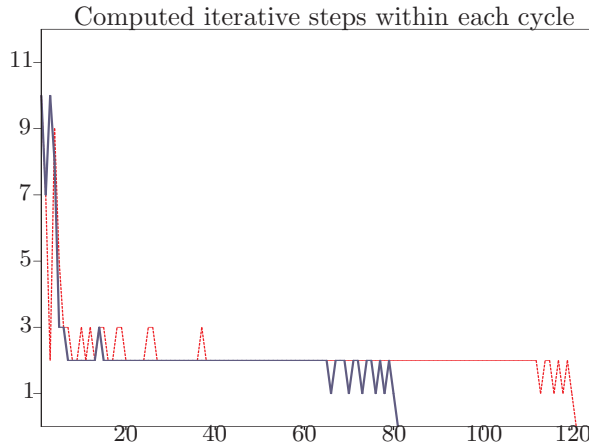


Figure 8: Comparison between the performance of L-SDK and L-LK methods. The solid (blue) line shows the actually performed number of steps within each cycle of the L-SDK method, while the dashed (red) line gives the corresponding information with respect to the L-LK method.

stopping rule for the L-SDK method is satisfied after 81 cycles. For the L-LK method, the same stopping criteria is reached only after 121 cycles. In order to obtain the same accuracy with the LK method, 380 cycles are required.

In the top pictures of Figure 7 one can see the iteration error for the L-SDK method after 10 and 81 cycles. For comparison purposes, the iteration error for the L-LK method is shown after 80 and 121 cycles (see the central pictures of Figure 7). The bottom pictures of Figure 7 show the iteration error for the LK method after 120 and 380 cycles. The number of actually computed iterative steps within each cycle of the L-SDK and L-LK methods is shown in Figure 8.

We provide a complete convergence analysis for the L-SDK iteration, proving that it is a convergent regularization method in the sense of [7]. Moreover, we prove a convergence result for the SDK iteration. From Theorem 3.3 follows that the SDK is a convergent method for exact data.

What concerns the numerical experiments for the inverse doping problem, the L-LK method requires almost 50% more cycles than the L-SDK method in order to reach the stop criteria (8). Moreover, the LK method requires almost three times more cycles than the L-LK method in order to achieve the same accuracy (see [10] for other comparisons between the LK and L-LK methods). The efficiency of the L-SDK method becomes even more evident when we compare the total number of actually performed iterative steps. Each cycle of the LK method requires the computation of 11 steps, while in the L-SDK and L-LK methods the number of actually performed steps per cycle is very small after a few number of cycles. As

one can see in Figure 8, no more than 2 steepest descent steps per cycle are computed after the 14-th cycle of the L-SDK method. Analogously, no more than 2 Landweber steps per cycle are computed after the 37-th cycle of the L-LK method. In total, for the computation of the LK-approximation in Figure 7 (380 cycles), 4180 Landweber steps are needed, while the L-LK-approximation (121 cycles) requires the computation of 258 Landweber steps and the L-SDK-approximation (81 cycles) requires the computation of 184 steepest descent steps.

6 Conclusions

In this paper we propose a new iterative method for inverse problems of the form (2), namely the L-SDK method. As a by-product we also formulated the SDK iteration, which is the steepest descent counterpart of the LK method [17].

In the L-SDK iteration we omit an update of the SDK iteration (within one cycle) if corresponding i -th residual is below some threshold. Consequently, the L-SDK method is not stopped until all residuals are below the specified threshold. The L-SDK method is the steepest descent counterpart of the L-LK iteration [11, 10].

Acknowledgments

The work of M.H. and O.S. is supported by the FWF (Austrian Science Fund) grants Y-123INF and P18172-N02. The work of A.L. and A.DC. are supported by the Brazilian National Research Council CNPq, grants 306020/2006-8 and 474593/2007-0. The authors thank Andreas Riederer for stimulating discussion on iterative regularization methods.

References

- [1] A. B. Bakushinsky and M. Y. Kokurin, *Iterative methods for approximate solution of inverse problems*, Mathematics and Its Applications, vol. 577, Springer, Dordrecht, 2004.
- [2] M. Burger, H. W. Engl, A. Leitão, and P.A. Markowich, *On inverse problems for semiconductor equations*, Milan J. Math. **72** (2004), 273–313.
- [3] M. Burger, H. W. Engl, P. A. Markowich, and P. Pietra, *Identification of doping profiles in semiconductor devices*, Inverse Problems **17** (2001), no. 6, 1765–1795.

- [4] M. Burger and B. Kaltenbacher, *Regularizing newton-kaczmarz methods for nonlinear ill-posed problems*, SIAM J. Numer. Anal. **44** (2006), 153–182.
- [5] Y. Censor, P.P.B. Eggermont, and D. Gordon, *Strong underrelaxation in kaczmarz’s method for inconsistent systems*, Numerische Mathematik **41** (1983), 83–92.
- [6] P. P. B. Eggermont, G.T. Herman, and A. Lent, *Iterative algorithms for large partitioned linear systems, with applications to image reconstruction*, Linear Alg. Appl. **40** (1981), 37–67. MR 84c:65059
- [7] H.W. Engl, M. Hanke, and A. Neubauer, *Regularization of inverse problems*, Kluwer Academic Publishers, Dordrecht, 1996.
- [8] D. Finch and Rakesh, *The spherical mean value operator with centers on a sphere*, Inverse Problems **23** (2007), no. 6, S37–S49.
- [9] M. Haltmeier and T. Fidler, *Frequency domain reconstruction in photo- and thermoacoustic tomography with line detectors*, arXiv:math.AP/0610155 (2007), submitted.
- [10] M. Haltmeier, R. Kowar, A. Leitão, and O. Scherzer, *Kaczmarz methods for regularizing nonlinear ill-posed equations. II. Applications*, Inverse Probl. Imaging **1** (2007), no. 3, 507–523.
- [11] M. Haltmeier, A. Leitão, and O. Scherzer, *Kaczmarz methods for regularizing nonlinear ill-posed equations. I. convergence analysis*, Inverse Probl. Imaging **1** (2007), no. 2, 289–298.
- [12] M. Hanke, *Conjugate gradient type methods for ill-posed problems*, Longman Scientific & Technical, 1995.
- [13] M. Hanke, A. Neubauer, and O. Scherzer, *A convergence analysis of Landweber iteration for nonlinear ill-posed problems*, Numer. Math. **72** (1995), 21–37.
- [14] M.R. Hestenes and E. Stiefel, *On the convergence of the conjugate gradient method for singular linear operator equations.*, J. Research Nat. Bur. Standards **49** (1952), 409436.
- [15] S. Kaczmarz, *Approximate solution of systems of linear equations*, Internat. J. Control **57** (1993), no. 6, 1269–1271, Translated from the German.
- [16] B. Kaltenbacher, A. Neubauer, and O. Scherzer, *Iterative regularization methods for nonlinear ill-posed problems*, de Gruyter, 2008, to appear.

- [17] R. Kowar and O. Scherzer, *Convergence analysis of a landweber-kaczmarz method for solving nonlinear ill-posed problems*, Ill posed and inverse problems (book series) **23** (2002), 69–90.
- [18] P. Kuchment and Kunyansky L.A., *Mathematics of thermoacoustic and photoacoustic tomography*, Eur. J. Appl. Math. (2007), at press.
- [19] L. Landweber, *An iteration formula for Fredholm integral equations of the first kind*, Amer. J. Math. **73** (1951), 615–624.
- [20] A. Leitao, P.A. Markowich, and J.P. Zubelli, *On inverse doping profile problems for the stationary voltage-current map*, Inv.Probl. **22** (2006), 1071–1088.
- [21] A.K. Louis and E.T. Quinto, *Local tomographic methods in sonar*, Surveys on solution methods for inverse problems, Springer, Vienna, 2000, pp. 147–154.
- [22] S. McCormick, *The methods of kaczmarz and row orthogonalization for solving linear equations and least squares problems in hilbert space*, Indiana Univ. Math. J. **26** (1977), 1137–1150.
- [23] V.A. Morozov, *Regularization methods for ill-posed problems*, CRC Press, Boca Raton, 1993.
- [24] F. Natterer, *The mathematics of computerized tomography*, SIAM, Philadelphia, 2001.
- [25] F. Natterer and F. Wübbeling, *Mathematical Methods in Image Reconstruction*, SIAM, Philadelphia, 2001.
- [26] Frank Natterer, *Algorithms in tomography*, State of the Art in Numerical Analysis, vol. 63, 1997, pp. 503–524.
- [27] G. Paltauf, R. Nuster, M. Haltmeier, and P. Burgholzer, *Experimental evaluation of reconstruction algorithms for limited view photoacoustic tomography with line detectors*, Inverse Problems **23** (2007), no. 6, S81–S94.
- [28] ———, *Photoacoustic tomography using a mach-zehnder interferometer as acoustic line detector*, Applied Optics (2007), 3352–3358.
- [29] O. Scherzer, *A convergence analysis of a method of steepest descent and a two-step algorithm for nonlinear ill-posed problems*, Numer. Funct. Anal. Optim. **17** (1996), no. 1-2, 197–214.
- [30] T.I. Seidman and C.R. Vogel, *Well posedness and convergence of some regularisation methods for non-linear ill posed problems*, Inverse Probl. **5** (1989), 227–238.

- [31] J.R. Shewchuck, *An introduction to the conjugate gradient method without the agonizing pain*, Tech. report, Scholl of Computer Science, Carnegie Mellon University, 1994.
- [32] A. N. Tikhonov and V. Y. Arsenin, *Solutions of ill-posed problems*, John Wiley & Sons, Washington, D.C., 1977, Translation editor: Fritz John.
- [33] A.N. Tikhonov, *Regularization of incorrectly posed problems*, Soviet Math. Dokl. **4** (1963), 1624–1627.
- [34] M. Xu and L.V. Wang, *Photoacoustic imaging in biomedicine*, Review of Scientific Instruments **77** (2006), no. 4, 041101.
- [35] Y. Xu, L.V. Wang, G. Ambartsoumian, and Kuchment P., *Reconstructions in limited-view thermoacoustic tomography*, Medical Physics **31** (2004), no. 4, 724–733.